Hindawi
Advances in Civil Engineering
Volume 2022, Article ID 6126823, 13 pages
https://doi.org/10.1155/2022/6126823

Research Article

Simulation-Based Tracking Test and Optimization of Large-Tonnage Box Girder Transport with Trolley on an Erected Bridge

Lei Wang[1,2] **Zhong-da Lv**[2] **Ai-min Xu**[3] **Fei Wang**[2] **and Xin-long Dong**[1]

[1]*MOE Key Laboratory of Impact and Safety Engineering, Ningbo University, Ningbo 315211, China*
[2]*Zhejiang Engineering Technology Research Center of Civil Engineering Industrialized Construction, Ningbo University of Technology, Ningbo 315211, China*
[3]*Ningbo Highway Construction Management Center, Ningbo 315100, China*

Correspondence should be addressed to Zhong-da Lv; lzd01@189.cn

Received 11 June 2021; Revised 9 May 2022; Accepted 24 May 2022; Published 11 June 2022

Academic Editor: Ankit Gupta

In the construction of large-tonnage box girder, the construction load of box girder transport is generally greater than the operating load in highway industry; therefore, it is a crucial task to carry out accurate simulation and optimization on bearing box girder. For this purpose, the refined modeling method of 40 m/1270t box girder is studied first in this paper, followed by detailed stress analysis by considering the impact coefficient of vehicles and the most unfavorable conditions. Tracking tests on dead load, prestressed load, and the transport load have shown that the calculated stress values obtained by the refined models are very close to the measured stress values. Based on dynamic strain test of the vehicles at the speed of 4 km/h, the impact coefficient of four vehicles is estimated to be 1.08 and its value meets the requirements of no more than 1.1 provided by the vehicle manufacturer. Aimed at no tensile stress in the midspan section, the optimized geometry of 40 m box girder is obtained with less concrete and longitudinal prestressed tendons. These results demonstrate the plausibility and validity of the proposed research methods and optimization schemes for large-tonnage box girder transport.

1. Introduction

For rapid construction and cost-saving, the prefabricated bridge technology is now in common use all over the world, which is mainly featured by standardization of bridge design, industrialization of component manufacturing, assembly construction, and informatization of management control [1], along with the development of bridge construction.

In industrialization, the large tonnage box girder has been widely used due to its large structural stiffness, fast construction speed, less joints, good durability, and easy maintenance [2]. In China, the large-tonnage box girders have been adopted in various projects like Hangzhou Bay Bridge, Donghai Bridge, and Jiaozhou Bay Bridge.

Large-tonnage precast box girder is generally designed in symmetrical form. It can be delivered to the erection sites via erected girders. The whole construction process has little impact on the ground traffic. In railway industry, 32 m/900 t box girders are generally transported by single vehicle along the left and right roof surface of bearing box girders [3, 4]. In highway industry, T-beams, small box girders, and others are mostly below 250 t [5]. However, for the transport of box girder weighing about 1000 tons, one of the most prominent characteristics is that the construction load of girder transport is generally greater than the operating load, which usually turns out to be the main control factor in the structural design of large tonnage box girder [6, 7].

Conservative design is usually adopted to ensure the safety and reliability of bearing box girder. Serving as a very important method, numerical simulation using finite element software package is widely used to carry out the simulation and optimization for different engineering

structures [8–10]. Fadi Oudah [11] studied the live-load factor and load combination for bridge systems conveying heavy mining trucks by SAP2000. The results indicate that the live-load factor can be 1.33 for mine haul trucks moving on short-span composite steel girders or NU precast girder bridge systems. However, the paper does not verify the impact coefficient of the actual conveying heavy mining trucks. Qin et al. [12–14] conducted research on the influence of different parameters of common engineering structures based on numerical models and optimization theory. The optimized structures can make full use of the bearing capacity of the material. The research provides effective scientific value for optimal design of engineering structure. Linear mechanical analysis is widely used in stress analysis of large tonnage concrete box girder, whose theory assumes that the relationship between stress and strain is linear in the process of loading and unloading. Xu et al. [15] studied the overall deformation and local stress near the simply supported section of 50 m concrete approach bridge of Hangzhou Bay Bridge via ANSYS. Yang et al. [16] established the beam element model of 40 m box girder of Meizhou Bay Bridge via BSAS and verified that temporary support can meet the requirements of 40 m concrete box girder transport. Nevertheless, both researcher groups have not conducted stress analysis on key midspan section. Fang et al. [17] established the beam element models and solid element models by using midas Civil and ANSYS, respectively. 35 m/800 t asymmetric box girder transport is simulated for different transport modes and bridge structure systems, which indicates that the mid-span bending moment of continuous girder is less than that of simply supported bridge. Meanwhile, large negative bending moment occurs at the fulcrum. More stress details can be obtained by using the solid element model. Deng et al. [18, 19] carried out the design optimization of 32 m and 40 m simply supported box beam on high-speed railway and obtained 40 m span box girder on high-speed railway with more economical deck width, web thickness, and beam height. It can expand the application scope of prestressed concrete simply supported beam bridge of high-speed railway. Although short of test verification, these research works provide a good idea for stress analysis and optimization of larger-tonnage box girder in highway.

During the fabrication and erection process, Bujnakova et al. [20, 21] used vibrating wire strain gauges to collect the stress and temperature data of the segmental precast box girder. It serves as an important way to ensure safety under the construction of bridges as well as the subsequent service period. Li [22] carried out tracking test on stress and deformation during the 530 t girder vehicle in phase 2 of Chengdu Metro line 10 passes through the steel trestle to transport the beams. According to the obtained changing state and law of the steel trestle, the construction countermeasures and measures are to ensure the safety of the steel trestle. Wang et al. [23] carried out the eccentric load test to simulate 32.5 m asymmetric box girder transport by using single 850 t girder vehicle. The maximum transport load is simulated by using 7 jacks according to moment equivalence in mid-span section. The stress and displacement increment law is obtained. It verifies the feasibility of the scheme to use a 850 t girder carrier. Although there are differences between the bridge types, load conditions, and measuring points layout, those research works provide various important test methods to obtain actual stress.

In engineering practice, there are still some problems to be solved for safety and cost-savings in the transport of large-tonnage box girder, especially for the box girder weighing about 1000 t. Due to the complexity and variety of practical engineering problems, it is necessary to develop a refined model and optimization scheme for those large-tonnage box girders [24, 25]. For this purpose, the fine modeling and optimization idea for 40 m large-tonnage box girders in Sanmen Bay Bridge of China are detailedly studied in this paper. The project overview and design of 40 m box girder transport with trolley on erected bridge are first introduced. The corresponding refined model is proposed to simulate the most unfavorable condition of box girder transport. The systematic tracking test is then carried out to verify the accuracy of the proposed modeling method. Dynamic strain test is conducted to obtain the actual impact coefficient of the vehicles. In the end, validated modeling method is used to optimize the geometry and prestressed tendons, which aims at no tensile stress in the mid-span section. New design of 40 m box girder is obtained with less concrete and longitudinal prestressed tendons. The refined models and field tests adopted in this paper are of great significance to obtain the accurate stress of large-tonnage box girder. The effectiveness scientific research value of refined models and optimization idea is verified by engineering examples.

2. 40 m Symmetrical Box Girder Transport with Trolley on an Erected Bridge

2.1. Project Overview. As a main cross-sea passage with six bidirectional lanes, Sanmen Bay Bridge connects Xiangshan Port Bridge and Taizhou Bay Bridge. The superstructure of the approach bridges is of concrete continuous girder structures applied with C50 high performance concrete. 40 m large-tonnage box girders are constructed with integral precast technology, with its width and height of 16.25 m and 2.6 m, respectively, and the height span ratio is 1 : 15.4. Box girder webs are inclined and the tilt is 1 : 3.8. The constant web thickness was determined by shear considerations, because of the presence of tendon ducts in the concrete. The thickness of web plate increases gradually from 50 cm and 70 cm to 110 cm within 12.95 m from the end, in order to meet the basic requirements for the construction load such as double-layer girder storage, girder transport, and erection, combined with the withdrawal requirement of comprehensive hydraulic internal formwork. The box segment has a bottom slab width of 7.65 m and the thickness is variable, which results from the limit deflection criteria under the live loading. The local haunches are used at the intersection of the bottom slab and the webs, aiming at providing sufficient space for accommodating the required number of tendon ducts. The weight of single box girder is about 1270 t. The typical longitudinal and cross sections are

shown inFigures 1–3. Without Figure 2 considering the dead load, the positive moment of mid-span section is 23119 kN m under the secondary dead load and operating load.

2.2. Design of Box Girder Transport with Trolley on the Erected Bridge. Aimed at conducting 40 m/1270 t box girder transport in Sanmen Bay Bridge, four vehicles are designed to form semirigid connections with synchronous control system. Single vehicle can move along the roof surface of the left or right bearing box girders, shown in Figure 4. The transverse wheel space is 6.5 m and 10.25 m, respectively. The upper box girder transport is carried out when the bearing box girder is in simple support state. For 40 m bearing box girder, the construction load mainly includes the dead load, prestressed load, the transport load of the vehicles, and upper box girder. The impact coefficient of vehicles should be considered in stress analysis.

In order to reduce the load effect of box girder transport, the transport load is shared by at least four bearing box girders. The wheel range of single vehicle should be controlled within 19.7 m, with the vehicle parameters of the axle number, wheelbase, and dead weight under consideration. When the wheelbase is 1.2 m and the number of axles is selected as 16, the weight of the whole vehicle is 550 t, which is relatively appropriate. The overall dimension of the whole vehicle is 53 m × 25.75 m × 4.3 m. It is obvious that when the wheel group center of front or the last two vehicles is located in the mid-span section, the longitudinal stress of bearing box girder is most unfavorable, as is shown in Figure 5. Under the transport load, the positive moment of mid-span section is 34110 kN m, which is obviously greater than the calculated moment of the secondary dead load and operating load. It verifies that the construction load of box girder transport is the main factor in this bridge design.

3. The Simulation Analysis of 40 m Bearing Box Girder

Finite element simulations of 40 m box girder are performed and the results will be used to determine the stress state of 40 m bearing box girder under the dead load, transport load, and prestressed load. All simulations are carried out using the statics solver of the finite element software package ADINA R9.6.0. The prestressed tendons are meshed with 2-node 3D Truss-rebar element with 3 translational degrees of freedom in each node, while other components (the box girder, cushion blocks, and supports) are meshed with reduced integration 8-node 3D-solid elements with stiffness-based hourglass control [26]. The spatial effect and friction loss of prestressing tendon are considered according to posttensioned hole friction loss test. Parameters k and μ are 0.00152 and 0.207, respectively. The bottom of the temporary bearings is simulated as rigid element. Modulus of elasticity for girder contact layer will not show tensile stress when rotations and deformations occur at girder end. Owing to the relatively sensitive change of the stress in mid-span section, a thicker element mesh is adopted for mid-span section.

Since the box girder was poured, three-stage construction of prestressed tendons has been carried out in about 48 h, 8 2h, and 320 h, respectively. Box girder transport test is carried out in about 1080 h, and corresponding laboratory tests have been carried out to obtain the actual elastic modulus at each important stage of 40 m box girder. Other parameters for concrete and prestressed tendons characteristics are determined based on specifications for the design of highway bridge (JTG 3362–2018) [27]. Material parameters in Table 1 are used in refined model for linear mechanical analysis of simply supported box girder.

In order to simulate the most unfavorable case of 40 m box girder transport precisely, cushion block without density is established in the designated top surface of bearing box girder. Two kinds of modeling methods are used in model 1 and model 2 based on the actual tire-ground contact area. One cushion block is established in model 1 to simulate the comprehensive effect of tires A and B, with single size of 0.497 m × 1.0 m × 0.3 m, as is shown in Figure 6. Two cushion blocks are established in model 2 to simulate tires A and B, respectively. The single size is 0.497 m × 0.5 m × 0.3 m. The mesh size of cushion blocks is 0.2485 m × 0.25 m × 0.15 m in two models.

When four vehicles are stationary, the loads of tire A and tire B are both 69.7 kN. When four vehicles carry the upper box girder along the erected box girder at low speed, it is assumed that the pressure of all tires is consistent and the impact coefficient effect can be considered as the increment of static loads. The pressure of the tires at corresponding position is converted to uniform pressure and applied to the upper surface of the cushion block.

Element mesh should be as subdivided as possible when the structure is discretized. Maximum and minimum sizes of model 1 along the girder length direction are 1.0 m and 0.2485 m, respectively. The maximum size occurs in the ranges of 5 m–16.7 m and 22.7 m–35 m, whereas the minimum size mainly appears near the cushion blocks. The mesh size within 6 m of mid-span section is 0.35 m. The maximum and minimum sizes of concrete elements along the box girder height direction are 0.3 m and 0.04 m, respectively. The maximum unit size appears in the web, whereas the minimum size appears in the edge of top plate. The maximum and minimum sizes of concrete elements along the box girder width direction are 0.475 m and 0.1 m, respectively, with the maximum unit size appearing in the top plate and the minimum size appearing in the web of mid-span section. The mesh size of prestressed tendons is 0.35 m. The total number of elements in model 1 is about 115,000, while 1,800 are used for the prestressed reinforcement. The total number of nodes is about 168,000. The mesh size control of model 2 is basically the same as that of model 1.

Before the stress analysis of 40 m bearing box girder, four other finite element models are established to study the influence of mesh size on the calculation results according to the same geometry of model 1. The mesh size is controlled according to about 0.5 times, 1.5 times, 2 times, and 2.5 times

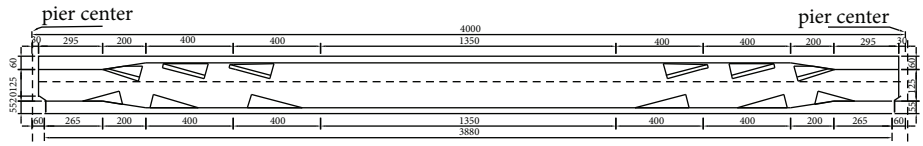

Figure 1: Longitudinal section of 40 m box girder (cm).

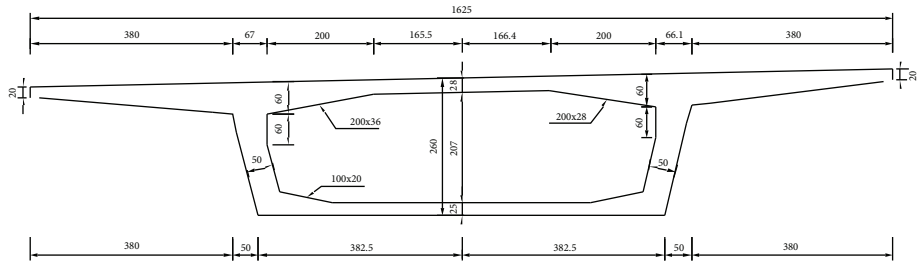

Figure 2: Mid-span section (cm).

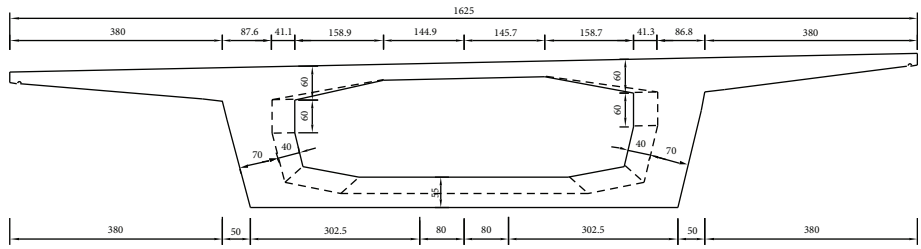

Figure 3: End section (cm).

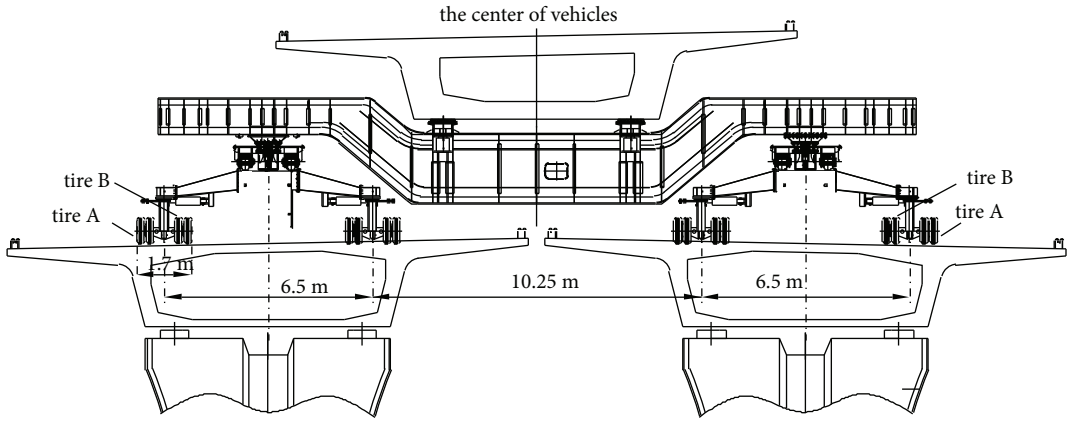

Figure 4: Box girder transport with four vehicles.

of model 1. Without considering the impact coefficient, the longitudinal stress increments of six models are basically the same in the bottom plates of mid-span section under the transport load. The differences at the same location are basically within 4.6%. However, excessive mesh size is more likely to lead to stress concentration near the cushion block of the top plate, which is disadvantageous to the accurate stress analysis of top plate. Smaller mesh size will increase the numbers of nodes, elements, and calculations significantly. The comparative stress results of key mid-span section in six models show that the mesh size from 0.5 times to 1.5 times has little impact on stress increment, and the mesh size selected in model 1 and model 2 is relatively reasonable. The mesh size of the subsequent calculation models is basically carried out based on this control range.

3.1. The Simulation of Dead Load. According to the sum of four support reactions in model 1 and model 2, the total weight of 40 m concrete box girder is 1270 t. By recording the amount of C50 concrete and reinforcement in prefabrication yard, the average weight of two box girders is 1264 t.

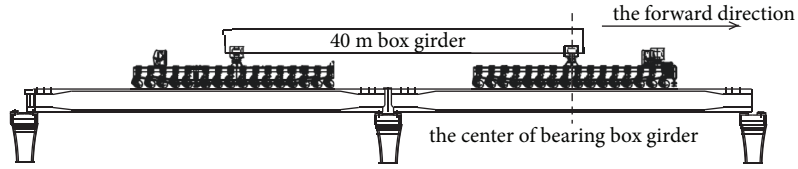

Figure 5: The most unfavorable condition of box girder transport.

Table 1: Material parameters.

C50 concrete Elastic modulus ($\times 10^4$ MPa)				Density (kg/m^3)	Prestressed tendons	
					Density (kg/m^3)	Elastic modulus (10^4 MPa)
48 h	82 h	320 h	1080 h	2650	19.5	7850
2.34	3.15	3.52	3.64			

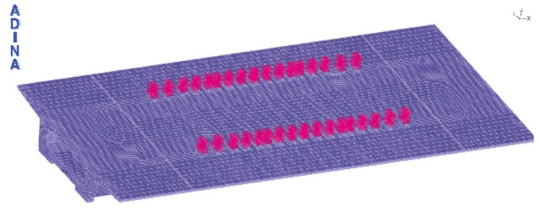

Figure 6: The finite element model of box girder transport.

Tracking test of single-layer box girder storage is carried out in the storage area. The total weight of 40 m box girder is tested by using four large bearing reaction meters of 500 t and its value is 1252 t. The data of these three groups of 40 m box girder weight are relatively close and the difference is within 2%. It is illustrated that the selection of material parameters is reasonable in model 1 and model 2 and that the structure model established by ADINA is able to simulate the actual situation of 40 m/1270 t precast box girder. Under the dead load, the images from stress result in mid-span section show that the tensile stress at the lower edge of bottom plate is 8.7 MPa~9.2 MPa and that the compressive stress at the upper edge of bottom plate is 4.6 MPa~5.5 MPa.

3.2. The Simulation of Transport Load. Taking model 1 for example, the longitudinal stress increment of the mid-span section under the transport load is shown in Figure 7 (the compressive stress increment is negative, and the tensile stress increment is positive, the same as below). For the key mid-span section, the stress distribution shows that the bottom plate is in the state of compressive stress increment, whereas the top plate is in the state of tensile stress increment. The tensile stress increment in lower edge of bottom plate is 5.1 MPa~5.7 MPa. The compressive stress increment in upper edge of bottom plate is 2.3 MPa~3.3 MPa. The stress increment of mid-span cross section caused by the transport load is relatively balanced, which conforms to the fact that both the box girder structure and transport mode are basically symmetrical.

On the basis of contrast analysis of the stress results caused by transport load, the longitudinal stress increment at the top plates and bottom plates of model 1 is basically consistent with that of model 2. Therefore, it can be inferred that the loads of tires A and B can be considered as a whole. Model 1 has easier benefits compared to model 2 and the accuracy of calculation results can also be guaranteed.

According to the data provided by the vehicle manufacturer, the impact coefficient is not more than 1.1 when the traveling speed of four vehicles is controlled within 4 km/h. So the impact coefficient of 1.1 times is considered in the maximum transport load. Under various load combinations, the lower edge stress increment of the mid-span section in model 1 and model 2 is shown in Table 2. For the combinations of the dead load and maximum transport load, the dead load effect accounts for more than 62% of the total load effect.

3.3. The Design and Simulation of Prestressed Load. Economic and reasonable prestressed tendon design is very important for large-tonnage box girder. According to the stress analysis of dead load and transport load, Figure 8 and Figure 9 give one feasible scheme of posttensioned prestressed tendons arrangement. The specific parameters are shown in Table 3.

For large-tonnage box girder, the construction of posttensioning method is divided into three stages. The first stage of posttensioning is performed on the precast pedestal to restrain the early crack caused by hydration heat of mass concrete. The compressive stress reserve of mid-span section shall not be less than 0.8MPa according to practical exploration of several engineering projects. To accelerate the turnaround efficiency of the precast pedestal, the second stage of prestressed tension is carried out on the precast pedestal to ensure that there is no tensile stress at the lower

Figure 7: Longitudinal stress increment of mid-span section caused by transport load (Pa).

Table 2: The lower edge stress increment of bottom plate in midspan section (MPa).

Load combinations	Dead load	Transport load	Maximum transport load	Dead load + maximum transport load
Model 1	8.7~9.2	5.1~5.7	5.6~6.3	14.4~15.2
Model 2	8.7~9.2	5.2~5.7	5.8~6.3	14.5~15.5

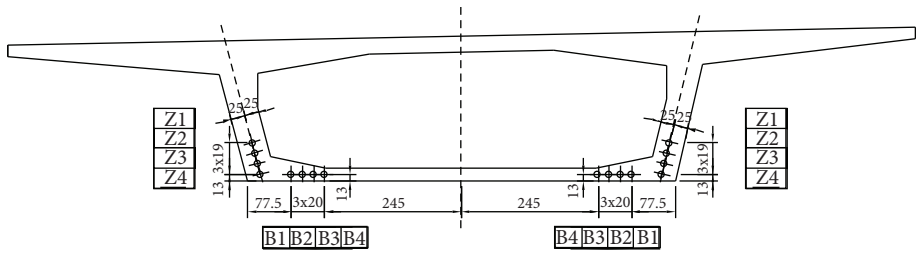

Figure 8: Prestress arrangement of the mid-span section (cm).

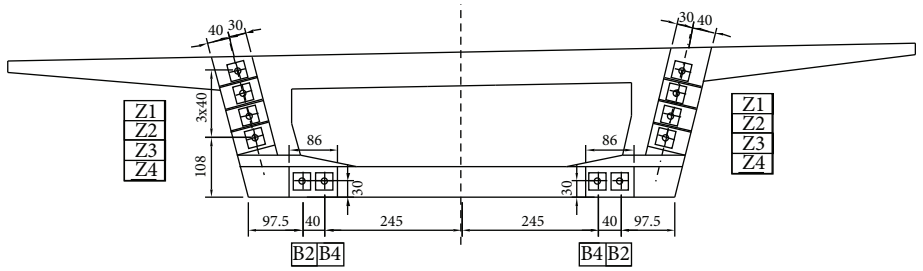

Figure 9: Prestress arrangement of the end section (cm).

Table 3: The design parameters of posttensioning method.

Number	Specification	Number of ducts	Bending angle (°)	Nominal area (mm^2)
Z1/Z2/Z3/Z4	19φ15.2	2 × 4 (long bundle)	6/6/6/6	140
B1/B3	15φ15.2	2 × 2 (short bundle)	5.3/5.3	140
B2/B4	19φ15.2	2 × 2 (long bundle)	6/6	140

edge of the bottom plate of the mid-span section during the lifting condition. The large-tonnage box girder is then moved to the storage area where the third posttensioning stage takes place. The stressing and grouting of all prestressed tendons in box girder were conducted in the storage yard before transport and erection. The control parameters of these three stages are designed in Table 4.

According to the stress results of simulating three-stage construction of posttensioned prestressed load, key mid-span section is in the state of compressive stress increment while under the dead load and prestressed load. The compressive stress increment in lower edge of bottom plate is 6.1 MPa~7.2 MPa, whereas the compressive stress increment in upper edge of top plate is 0.9 MPa~2.2 MPa. The maximum transport load is then applied to the model as the increment of static loads. Under the dead load, prestressed load, and maximum transport load, the key mid-span section is compressed without tensile stress. The stress increment in lower edge of bottom plate is 0.5 MPa~1.4 MPa. It is obvious that the 40 m bearing box girder is safe under the most unfavorable condition of box girder transport.

4. Tracking Test of 40 m Bearing Box Girder

4.1. Arrangement of Stress Measuring Points. In order to verify the accuracy of numerical simulation, the longitudinal

Table 4: The control parameters for three-stage construction of prestressed tension.

Number	Specification	Number of holes	Anchorage stress of prestressed tension (MPa)	Minimum strength requirement of concrete (MPa)
1	N2–B4	4	930	25
2	N4–N1–B3–N3–B1	10	930	40
3	N2–N4–B4–N1–B3–N3–B2–B1	16	1395	50

stress increment of two bearing box girders was tracking tested in actual construction process. Both the bearing box girders and transported box girders are selected as 40 m. Based on the stress analysis, Figure 10 gives five key control sections of two bearing box girders. The measuring points are arranged at the upper edge of the top plate and the lower edge of the bottom plates. The measuring points diagram and the field loading test of box girder transport are shown in Figures 11(a) and 11(b).

There are 50 stress measuring points for each test box girder. The vibrating wire strain sensor of Changsha Jinma Co., Ltd. is used in this test and it can measure strain increment and temperature changes accurately in specified location of box girder concrete. Its strain measuring range is $\pm 1500\ \mu\varepsilon$ the sensitivity is $0.1\ \mu\varepsilon$, the temperature range is -20–60°C, and the sensitivity is 0.1°C. All strain sensors are embedded at the designated position before the concrete casting.

The initial strain value and the initial temperature value were ε_0 and T_0, respectively. When the working condition changed, the measured strain value and temperature value were ε_1 and T_1, respectively. According to temperature correction, the measured stress increment values can be calculated as follows:

$$\sigma = E \times \left[\varepsilon_1 - \varepsilon_0 + 2.2 \times \left(T_1 - T_0\right)\right]. \quad (1)$$

Here, E is the elastic modulus of concrete.

4.2. Tracking Test of the Dead Load and Prestressed Load. The main purpose of this test is to obtain the real stress increment under the dead load and prestressed load. For three stages of posttensioning construction, Figure 12 presents cumulative stress increment of five measuring points at the bottom plate of key mid-span section. Mid-span section in the three stages is all in the state of compressive stress increment. Compared to the posttensioned prestressed construction at the first stage and the second stage, the compressive stress increment increases obviously in the third stage because the prestress effect in the first two stages is mainly used to offset the dead load of the box girder and the compressive stress reserve resisting the maximum transport load effect is mainly generated by the increment of the third stage. The trend of compressive stress increment is consistent with the objectives for the design. It can be considered that the tensioning scheme of three-stage prestress is reasonable.

After the third stage of construction, cumulative stress increment in lower edge of bottom plate is 6.4 MPa~6.8 MPa. These values are close to the corresponding values calculated in model 1 (6.1 MPa~7.2 MPa). It is illustrated that the refined model of dead load and prestressed load can be considered as a reliable tool for stress analysis.

4.3. Tracking Test of the Transport Load. The main purpose of this test is to obtain the real stress increment under the transport load. The stress measuring points arrangement is the same as that of the tracking test of dead load and prestressed load. Two transport cases are as follows: In Case 1, the wheel group center of the front two vehicles is located in the mid-span section of test box girder. In Case 2, the wheel group center of the last two vehicles is located in the mid-span section of test box girder. The vehicles reach the designated location in turn, followed by stress collection 10 minutes later.

Figure 13 presents the stress increment of key mid-span section in Case 1 and Case 2 of two test box girders. For the first bearing box girder, the stress increment values of Case 1 at the corresponding position are basically close to those of Case 2. They are verified for a second time in the second bearing box girder. Based on the almost same stress increment in Case 1 and Case 2 of the two test box girders, it can be inferred that the actual tire pressures of the front and last two vehicles are the same and that the design of four vehicles is successful in ensuring the consistency of tire pressure.

Taking Case 1 for example, Figure 14 presents the comparison of the measured stress increment values and the corresponding calculated values along the girder length direction. The measured stress increment is very close to the calculated stress in five key control sections. The stress values at corresponding position of the symmetrical sections, such as S1 and S5, as well as S2 and S4, are basically close to each other, which shows that the established refined model can simulate the most unfavorable condition of 40 m box girder transport. It also indicates that the stress increment of the mid-span section is obviously larger than those of other sections. Stress analysis on mid-span section should be more accurate.

Figure 15 presents the comparison of the measured stress increment values and the corresponding calculated values in key mid-span section. For the key mid-span section of the first test box girder, the measured stress increments of bottom plate and top plate are 4.96–5.52 MPa and -2.78~-3.54 MPa, respectively. The stress increment values at the corresponding position of the second bearing box girder is 5.16~5.66Mpa and -2.83~-3.28 MPa. The stress distribution is relatively balanced and there is no obvious shear lag effect in the top plate and bottom plate. 10 minutes after the vehicles leave the test box girder, the

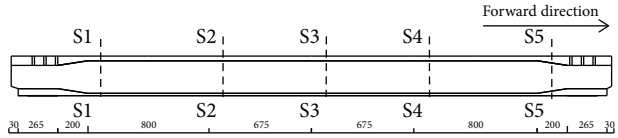

Figure 10: Critical control section of test box girders (cm).

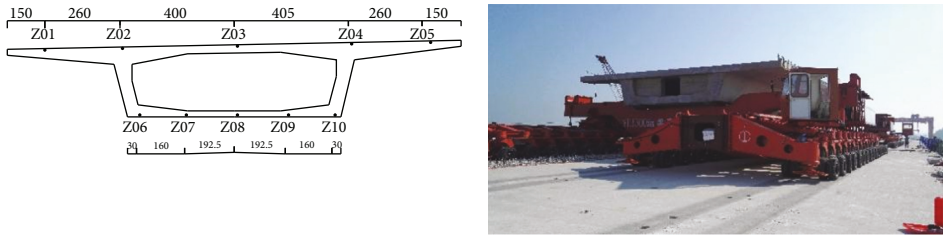

(a) (b)

Figure 11: Tracking test of 40 m bearing box girder. (a) Stress measuring points arrangement (cm). (b) The field loading test.

residual strain is collected. Relative residual strain of 10 measuring points in mid-span section is less than 5% and it also includes the measurement deviation of dynamic strain sensors. It shows that the box girder structure is still in the elastic range.

4.4. Dynamic Strain Test of the Transport Load. The main purpose of this test is to obtain the real stress increment under actual transport load. The dynamic strain sensor of Jiangsu Donghua Co., Ltd. is used in this test. It can measure the dynamic strain increment accurately in specified location of box girder concrete, with the strain measuring range of $\pm 3000\ \mu\varepsilon$ and the sensitivity of $0.1\ \mu\varepsilon$. It can operate normally in the range of -20°C to 80°C.

Dynamic strain measuring points are arranged at S3-Z08 and S3-Z10 of first test box girder. When the four vehicles pass through the 40 m bearing box girder at the speed of 4 km/h, the dynamic strain at the mid-span section is collected under the nonstop condition, with the total test time of about 109 s. By elastic modulus conversion, Figure 16 presents the dynamic stress increment of S3-Z08 and S3-Z10.

As Figure 16 indicates, the maximum dynamic stress increment of S3-Z10 is 6.01 MPa and it occurs in 28 seconds. It is the time during which wheel group center of front two vehicles travels to the mid-span section. When the wheel group center of the last two vehicles is traveling in the mid-span section, the maximum dynamic stress increment of S3-Z10 is 5.94 MPa. The stress increment values under the two working conditions are basically close and the difference is less than 2%. For another dynamic strain measuring point of S3-Z08, the maximum dynamic stress increments are 5.77 MPa and 5.64 MPa, respectively, and the difference is less than 3%. It is proved again that the tire pressure of the vehicles is basically consistent.

Under the transport load, the calculated stress increment of S3-Z10 is 5.54 MPa in model 1, and the ratio of maximum dynamic stress increment and 5.54 MPa is 1.085. The same analysis method was used for S3-Z08 and the ratio is 1.076.

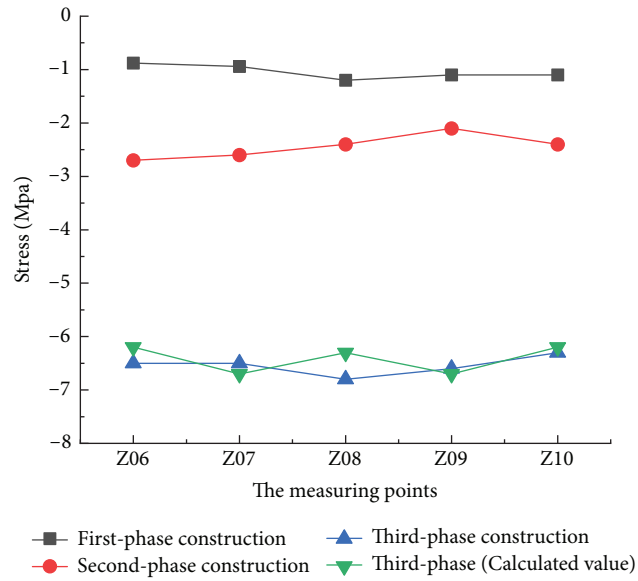

Figure 12: Stress increment comparison of the mid-span section.

The actual impact coefficient of the vehicles is estimated to be 1.08 according to the average value. Both impact coefficients obtained by dynamic strain test are less than 1.1. It is indicated that the design of the vehicles is successful in terms of impact coefficient. When carrying out 40 m box girder transport with trolley on erected bridge, it is suggested that the speed of four vehicles should be controlled within 4 km/h. It is relatively safe when using the impact coefficient provided by the manufacturer to design the large-tonnage box girder.

When the vehicles leave the test box girder, the dynamic strain increment is quickly reduced to a very small range. The relative residual strain of the two measuring points is less than 4% and it also includes the measurement deviation of dynamic strain sensors. According to the dynamic strain test results, the box girder structure is still in the elastic range. It is suitable to this study that the impact coefficient effect is considered as the increment of static loads.

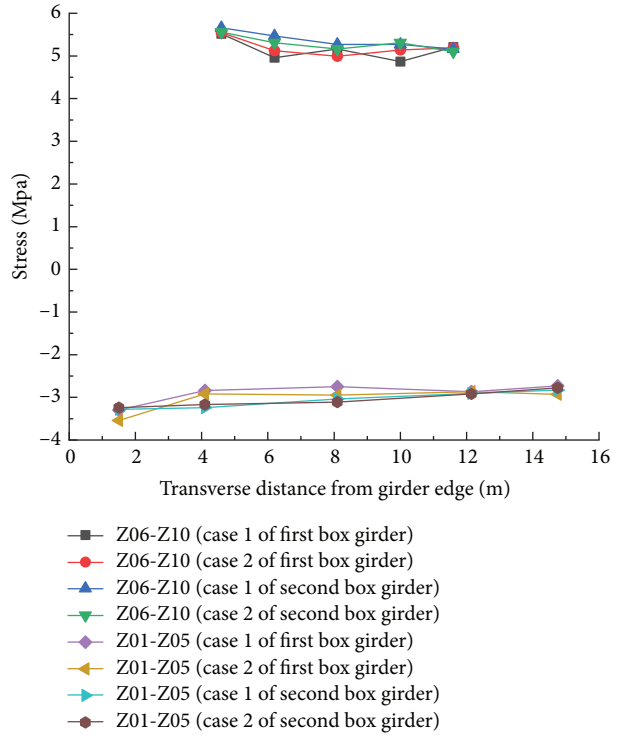

Figure 13: Stress increment comparison of Case 1 and Case 2.

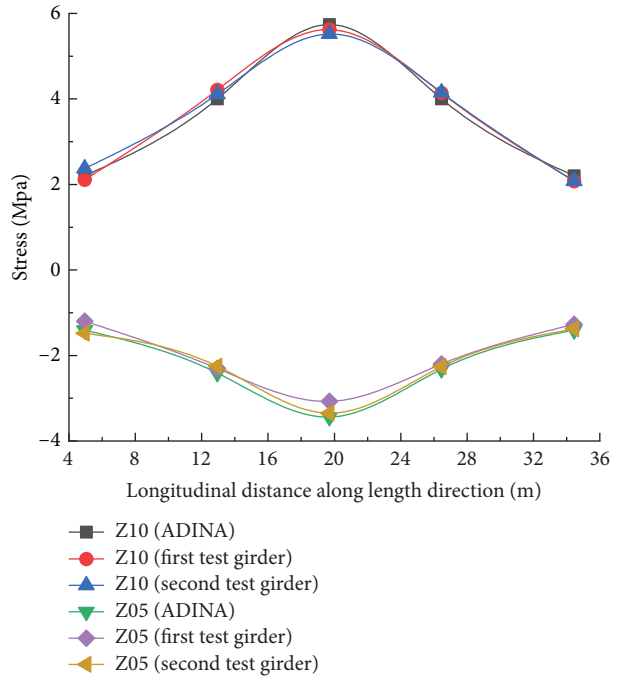

Figure 14: Stress increment along the girder length direction.

5. More Application Cases of Refined Modeling Methods

5.1. Numerical and Experimental Comparison of 32.5 m Asymmetric Box Girder. In order to study the suitability of the refined modeling method to other length box girders, a modeling method the same as above is adopted to analyze the eccentric load test of simulating 32.5 m/733 t box girder transport in [23]. There are 7 cushion blocks without density established to simulate the loading points of seven jacks, with the center distance of 3.856 m and the size of one cushion block of 0.33 m × 1.28 m × 0.3 m. Taking 1.1 times of

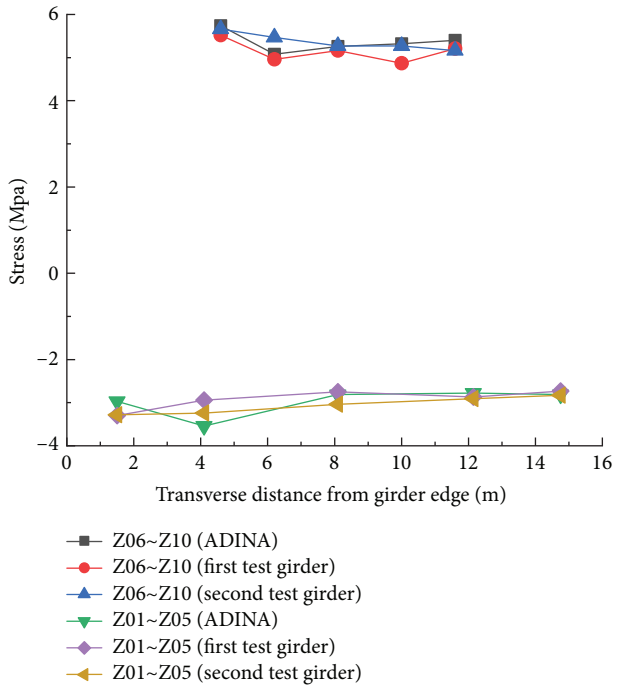

Figure 15: Stress increment of the mid-span section.

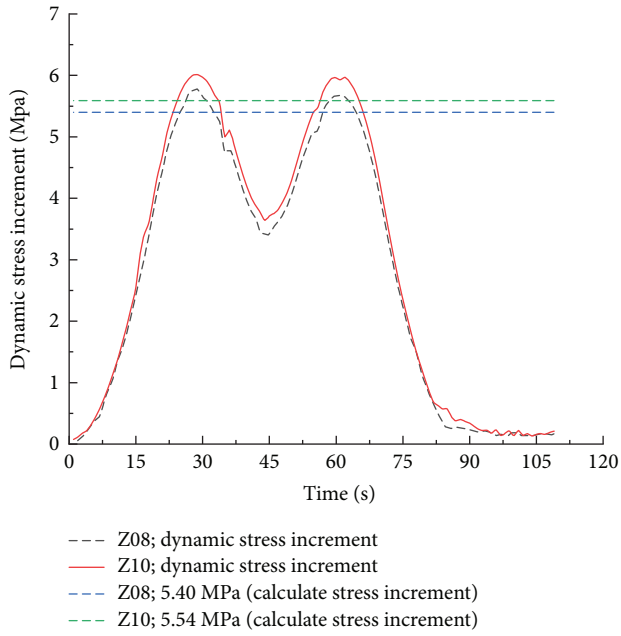

Figure 16: Dynamic stress increment of the first test box girder.

the impact coefficient into account, the load on single cushion block is 569 KN. Figure 17 presents the geometry of mid-span section and five control sections have the same measuring points layout.

Figure 18 shows the stress comparison along the girder length direction under the maximum transport load. The calculated values of Z01–Z04 are close to the test values, which illustrates that the corresponding refined model can also simulate 32.5 m asymmetric box girder transport. It is difficult to carry out field test for each practical engineering owing to the high cost. The above-validated modeling method provides an economical and reliable way to obtain the accurate stress of more box girders, especially in the phase of designing.

So far, the approaches of simulation analysis proposed above have been adopted in Sanmen Bay Bridge, Yuci Expressway, the second passageway of Hangzhou-Ningbo coastal expressway, and other numerous major bridge projects in China, which guarantees the applicability and reliability of large-tonnage box girder.

5.2. Geometry Optimization of 40 m Box Girder. According to the stress analysis on dead load and maximum transport load in Sanmen Bay Bridge demonstrated above, the dead load effect of bearing box girder accounts for more than 62% of the total load effect. It is obvious that reducing dead load by optimizing geometry is an effective way to reduce the total construction load.

For large-tonnage box girder in highway, it is difficult to adjust the girder height and the cantilever length because the bridge decking width is unchangeable. In middle standard section, the thickness of web is 50 cm and that of the bottom plates is 25 cm, which were determined by shear considerations, as tendon ducts internal to the concrete were present. The number of the prestressed tendons per web plate should not exceed 4×19 according to the limitation of the girder height and local stress in anchorage zone. Therefore, it is the preferred scheme to adjust the width of the bottom plate. According to the engineering practice, the reasonable and economical web plate tilt of symmetrical box girder should be controlled between 1 : 3 and 1 : 4.5.

Aimed at minimizing project cost, the vehicles in Sanmen Bay Bridge can be reused. With the application of the proposed modeling method mentioned above, new calculation model of optimized geometry can be established and applied for evaluating the safety and economy of 40 m box girder. Three phases for the optimizationprocess are asfollows:

(i) *Cross-Sectional Optimization*. The same modeling method is used to establish three models of different bottom plate width, to analyze the influence rule of bottom plate width on the stress of 40 m large tonnage box girder. The bottom plate widths of model 3, model 4, and model 5 are 7.6 m, 7.3 m, and 7.0 m, respectively. On the basis of keeping same prestressed tendons, the compressive stress of the bottom plate in key mid-span section increases gradually, whereas the bottom plate width decreases. When the bottom plate width is reduced from 7.65 m to 7.0 m, the weight can be effectively reduced from 1270 t to1242 t. The web plate tilt is adjusted from 1 : 3.8 to 1 : 3.4 and the value is still within the reasonable and economical range.

(ii) The web thickness design for the end section in large-tonnage box girder should not only meet the bending and shear requirements but also provide sufficient torsional stiffness. Based on the stress results of model 3, model 4, and model 5, the shear

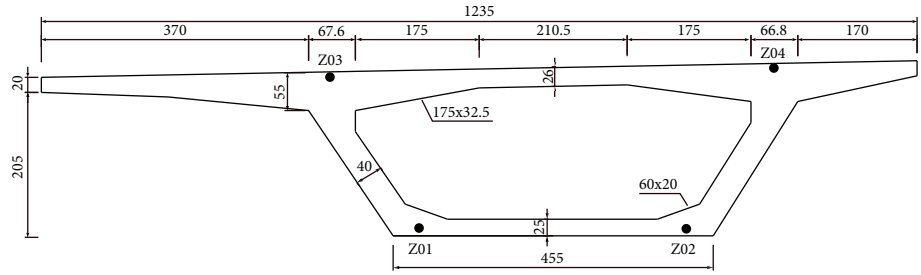

Figure 17: Stress measuring points arrangement of the mid-span section (cm).

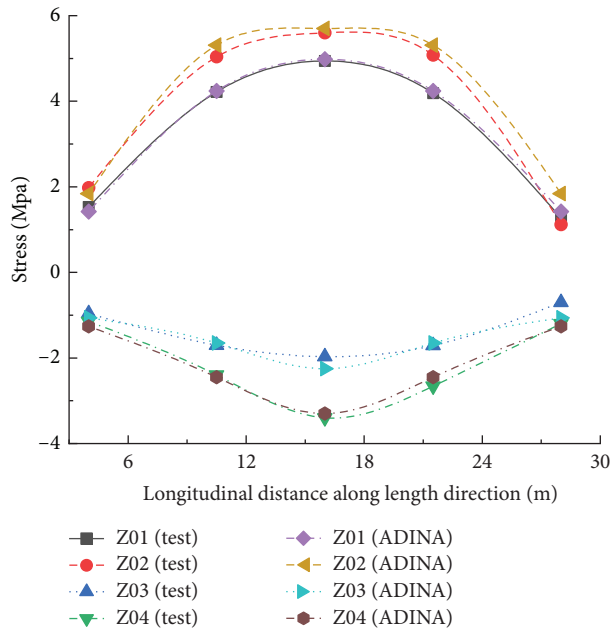

Figure 18: Stress increment along the girder length direction.

near the end section also decreases as the geometry and weight of box girder change. Model 6 with the web thickness of 100 cm and model 7 with the web thickness of 90 cm are established. The analysis results show that the web plate thickness can be further optimized from 110 cm to 100 cm.

(iii) *Longitudinal Section Optimization*. Based on the optimized cross section of model 6, model 8 is established and the longitudinal length of transition section is 2.95 m, 2.0 m, 3.0 m, and 3.0 m, respectively. The analysis results show that model 8 has great advantages both in cost and in mechanical performance. Figures 19 and 20 present the optimized longitudinal section and mid-span section of model 8. By optimizing the longitudinal section, the weight of 40 m box girder can be further reduced from 1242 t to 1222 t.

(iv) *Prestressed Tendon Optimization*. Keep the total number of prestressed tendons constant, and the mid-span section of model 8 is always in the state of compressive stress under the dead load, the maximum transport load, and prestressed load. The minimum compressive stress occurs at the lower edge of the bottom plate and its value is 1.3 MPa. The minimum compressive stress is too conservative and can be further reduced to nearly 0 MPa.

In order to control the minimum compressive stress of mid-span section, different combinations of prestressed tendon are considered in model 8. If deducting the prestressed tendon of B3 or B4, two sets of internal concrete tooth blocks in box girder can also be reduced. The total weight of 40 m box girder can be further reduced from 1222 t to 1220 t. When deducting the prestressed tendon of B4, under the dead load, the maximum transport load, and the optimized prestressed load, tensile stress of 0.2 MPa occurs on the bottom plate of the mid-span section. It goes beyond the design principle of controlling no tensile stress in key mid-span section of large-tonnage concrete box girder. Similarly, if deducting the prestressed tendon of B3, under the dead load, maximum transport load, and optimized prestressed load, the minimum compressive stress occurs at the lower edge of the bottom plate and its value is 0.2 MPa, as is shown in Figure 21.

Finally, it is appropriate to deduct the prestressed tendon of B3, the compressive stress reserve is enough, and it can still meet the safety requirements of 40 m box girder transport with trolley on erected bridge. Compared with 40 m/1270 t

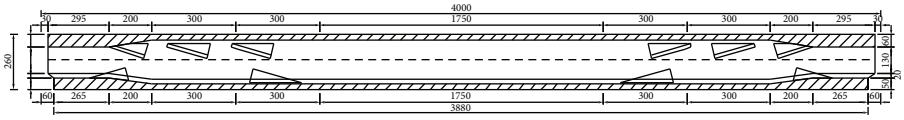

Figure 19: Longitudinal section of optimized 40 m box girder (cm).

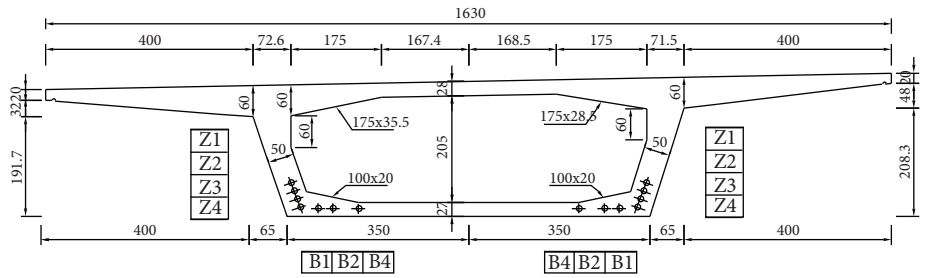

Figure 20: Mid-span section of optimized 40 m box girder (cm).

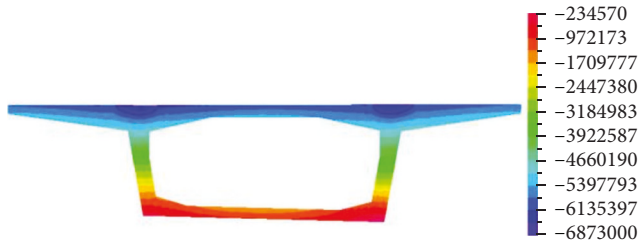

Figure 21: Longitudinal stress in the mid-span section of optimized 40 m box girder (Pa).

box girder in Sanmen Bay Bridge, single-optimized box girder can help to save 20 m^3 concrete and 2×15 prestressed tendons. In addition, reducing two sets of internal concrete tooth blocks is conducive to the pulling out of the internal formwork. Moreover, the prestressed tensioning efficiency is also greatly improved. At present, the optimized 40 m box girders and transport method have been adopted by the second passageway of Hangzhou-Ningbo Coastal Expressway. The ideas of geometry optimization for large-tonnage box girder were also applied in other similar projects in China, all achieving good economic and social benefits.

6. Conclusion

(1) For 40 m box girder transport, the refined models are established and the corresponding stress of key mid-span section is obtained under the dead load, prestressed load, and transport load. According to the proposed prestressed tendons design, there is still 0.5~1.4 MPa compressive stress at the lower edge of the bottom plate under the most unfavorable condition.

(2) Tracking test is carried out in the construction process. The actual stress increments under the dead load, prestressed load, and the transport load are obtained. The value is in consistency with the calculated value of ADINA finite element, which verifies the accuracy of refined models.

(3) The dynamic strain test results show that tire pressure is consistent. The actual impact coefficient is obtained to be 1.08 and its value meets the requirements of no more than 1.1 provided by the vehicle manufacturer. According to relative residual strain, the box girder is still in the elastic range under the most unfavorable condition. It is reasonable to consider the impact coefficient as the increment of static loads.

(4) In terms of security and economy, validated modeling method is applied to optimize the geometry and prestressed tendons. New design of 40 m box girder is obtained with less concrete and longitudinal prestressed tendons.

(5) The refined models, test methods, and optimization idea discussed in this study are helpful for the construction of the bridge, which may serve as a reference to the development of large-tonnage box girder designs to be more economical and less conservative. This research results are also suitable for larger span box girder, asymmetric box girder with large cantilever, and small radius curved box girder. Due to the fact that same vehicles are reused in the actual projects, the optimization research on different vehicles is not covered in this

study, which can be discussed in detail in the future research.

Data Availability

The data used to support the findings of this study are available from the corresponding author upon request.

Conflicts of Interest

The authors declare no conflicts of interest.

Acknowledgments

The authors gratefully acknowledge the financial supports from the National Natural Science Foundation of China (11390361) and Major Project of "Science and Technology Innovation 2025″ in Ningbo (2019B10076).

References

[1] M. Rettinger, A. Huckler, and M. Schlaich, "Technologies and developments in precast segmental bridge construction," *Beton- und Stahlbetonbau*, vol. 116, no. 2, pp. 12–23, 2021.

[2] A. A. Nassr, H. H. Abd-el-Rahim, F. Kaiser, and A. Eh El-sokkary, "Topology optimization of horizontally curved box girder diaphragms," *Engineering Structures*, vol. 256, Article ID 113959, 2022.

[3] X. H. He, T. Wu, Y. F. Zou, Y. F. Chen, H. Guo, and Z. Yu, "Recent developments of high-speed railway bridges in China," *Structure and Infrastructure Engineering*, vol. 13, no. 12, pp. 1584–1595, 2017.

[4] Y. Z. Zhou, L. J. Chen, and C. Gao, "Design technique and exploration of high-speed railway bridges in China," *Bridge Construction*, vol. 48, no. 5, pp. 11–15, 2018.

[5] M. O. F. Murad, Z. Chik, A. Mustafa, B. M. N. Absar, K. H. Shikdar, and K. A. M. Nayan, "A comparative study between structural properties of pre-tensioned inverted T-girder and actual post-tensioned box girder in bridge construction," *KSCE Journal of Civil Engineering*, vol. 20, no. 6, pp. 2403–2409, 2016.

[6] V. Torralba, T. Polo, G. Ramos, and A. Aparicio, "Design and construction of post-tensioned concrete box-girder viaducts for high-speed rail," *Proceedings of the Institution of Civil Engineers - Bridge Engineering*, vol. 173, no. 3, pp. 168–178, Article ID 00028, 2020.

[7] Y. Q. Xiang, S. Zhu, and Y. Zhao, "Research and development on accelerated bridge construction technology," *China Journal of Highway and Transport*, vol. 31, no. 12, pp. 1–27, 2018.

[8] M. Mawlana and A. Hammad, "Simulation-based optimization of precast box girder concrete bridge construction using full span launching gantry," in *Proceedings of the 4th Construction Specialty Conference, CSCE 2013 Annual Meeting*, Moncton, Canada, June 2013.

[9] P. Lazzari, A. Campos, and B. Lazzari, "Structural analysis of a prestressed segmented girder using contact elements in ANSYS," *Computers and Concrete*, vol. 20, no. 3, pp. 319–327, 2017.

[10] F. Erdal, O. Tunca, S. Tas, and R. Ozcelik, "Experimental and finite element study of optimal designed steel corrugated web beams," *Advances in Structural Engineering*, vol. 24, no. 9, Article ID 136943322098609, 2021.

[11] F. Oudah, G. Norlander, and R. El-Hacha, "Live-load factor and load combination for bridge systems conveying extremely heavy mining trucks," *Journal of Bridge Engineering*, vol. 22, no. 4, p. 1, Article ID 0000994, 2017.

[12] Y. X. Qin, Z. Q. Zhang, J. P. Gu et al., "Customized non-uniform discrete variables coordinated optimization coupling nonlinear mechanical analysis on complex truss structure," *Iranian Journal of Science and Technology, Transactions of Mechanical Engineering*, vol. 11, 2021.

[13] Y. Y. Zhang, Y. X. Qin, J. P. Gu et al., "Topology optimization of unsymmetrical complex plate and shell structures bearing multicondition overload," *Journal of Mechanical Science and Technology*, vol. 35, no. 8, pp. 3497–3506, 2021.

[14] J. P. Gu, Y. X. Qin, Y. Y. Xia et al., "Research on dynamic characteristics of composite towering structure," *International Journal of Applied Mechanics*, vol. 13, no. 08, Article ID 2150096, 2021.

[15] A. M. Xu, H. Z. Chen, and Z. C. Zhang, "Simulation analysis of girder transport process on the box girder of Hangzhou bay bridge," *China Railway Science*, vol. 05, pp. 22–25, 2005.

[16] T. H. Yang, L. Zhang, and H. Yang, "Design of box girder in 40m long simply-supported spans of approach bridges of meizhou bay sea-crossing bridge," *World Bridge*, vol. 48, no. S1, pp. 22–26, 2020.

[17] H. Fang, W. H. Jia, and L. T. Chen, "Scheme comparison of box girder transport with trolley on erected bridge on land highway," *Journal of China & Foreign Highway*, vol. 40, no. 2, pp. 155–160, 2020.

[18] Y. Q. Deng, S. Q. Xu, and J. J. Hou, "Design optimization of simply-supported box beam on high-speed railway," *Railway Standard Design*, vol. 63, no. 5, pp. 71–75, 2019.

[19] X. L. Ban, Y. H. Su, and N. Zhang, "Design parameters research on 32m simple-supported girder of newly built high speed railway with speed of 400km/h," *Railway Engineering*, vol. 58, no. 6, pp. 5–7, 2018.

[20] P. Bujnakova, "Construction of precast segmental box girder bridge," *IOP Conference Series: Materials Science and Engineering*, vol. 385, p. 1, Article ID 012007, 2018.

[21] F. Moreu, R. E. Kim, and B. F. Spencer, "Railroad bridge monitoring using wireless smart sensors," *Structural Control and Health Monitoring*, vol. 24, no. 2, p. 1, Article ID 1863, 2016.

[22] K. Z. Li, "Research on monitoring technology of bailey beam trestle bridge under the action of 500t girder transportation vehicle," *Railway Construction Technology*, vol. 6, pp. 96–104, 2020.

[23] F. Wang, Z. D. Lv, and A. M. Xu, "Test of eccentric delivery of girder undertaken by a single girder carrier traveling on separated twin asymmetric precast box girders," *Bridge Construction*, vol. 47, no. 6, pp. 66–71, 2017.

[24] R. Gaspar and F. R. Stucchi, "Web design of box girders concrete bridges," *Engineering Structures*, vol. 57, pp. 267–275, 2013.

[25] M. A. Haider, M. Batikha, and T. Elhag, "Precast versus cast in-situ concrete in the construction of post-tensioned box-girder bridges: span effect," *Structural Concrete*, vol. 21, no. 1, pp. 56–64, Article ID 201800263, 2020.

[26] Adina, "ADINA system online manuals," 2020, http://www.adina.com/adina-structures.shtml.

[27] Cccc Highway Planning, *Design institute, "JTG 3362-2018, specification for design of highway reinforced concrete and prestressed concrete bridge and culverts,"* The People's Communication Publishing Company, Beijing, China, 2018.